

De novo domestication of wild tomato using genome editing

Agustín Zsögön^{1,7}, Tomáš Čermák^{2,6,7}, Emmanuel Rezende Naves¹, Marcela Morato Notini³, Kai H Edel⁴, Stefan Weinl⁴, Luciano Freschi⁵, Daniel F Voytas², Jörg Kudla⁴ & Lázaro Eustáquio Pereira Peres³

Breeding of crops over millennia for yield and productivity¹ has led to reduced genetic diversity. As a result, beneficial traits of wild species, such as disease resistance and stress tolerance, have been lost². We devised a CRISPR–Cas9 genome engineering strategy to combine agronomically desirable traits with useful traits present in wild lines. We report that editing of six loci that are important for yield and productivity in present-day tomato crop lines enabled *de novo* domestication of wild *Solanum pimpinellifolium*. Engineered *S. pimpinellifolium* morphology was altered, together with the size, number and nutritional value of the fruits. Compared with the wild parent, our engineered lines have a threefold increase in fruit size and a tenfold increase in fruit number. Notably, fruit lycopene accumulation is improved by 500% compared with the widely cultivated *S. lycopersicum*. Our results pave the way for molecular breeding programs to exploit the genetic diversity present in wild plants.

Tomato (*S. lycopersicum*) is the most important vegetable fruit worldwide, with annual production of 100 million tons³. The domestication process from the putative ancestral progenitor, *S. pimpinellifolium*, which produces pea-sized fruits, to modern tomato varieties is well described⁴. However, despite the increases in yield conferred by domestication, the breeding focus on yield has been accompanied by a loss of genetic diversity and reduced nutritional value and taste⁵.

Many domestication traits have Mendelian inheritance patterns and involve loss-of-function or gain-of-function mutations⁶ (Table 1 and Supplementary Table 1). This means that it should be possible to recreate these traits in a suitable genetic background with CRISPR–Cas9 genome editing technology⁷. Although the first CRISPR–Cas9 applications created deletions, modern variants of CRISPR-based genome editing technologies can produce targeted insertions, exchange amino acids and modulate gene expression. Therefore, genome editing could be used to domesticate wild plants and reunite lost but desirable traits, including nutritional features or stress tolerance, with yield potential and other agronomically valuable characteristics⁸.

We previously identified a suite of loci that have shaped the morphology and agronomic potential of current cultivars of tomato, maize, rice and other crops and proposed a reverse genetic approach for the *de novo* domestication of novel crops⁹ (Table 1 and Supplementary Table 1). In tomato, at least six loci important for key domestication traits have been identified: general plant growth habit (*SELF-PRUNING*)¹⁰, fruit shape (*OVATE*)¹¹ and size (*FASCIATED* and *FRUIT WEIGHT 2.2*)^{12,13}, fruit number (*MULTIFLORA*)¹⁴, and nutritional quality (*LYCOPENE BETA CYCLASE*)¹⁵. We set out to create a novel crop derived from *S. pimpinellifolium* by targeting this set of genes using a multiplex CRISPR–Cas9 approach to generate loss-of-function alleles. We constructed a single CRISPR–Cas9 plant transformation vector, pTC321 (Supplementary Note 1), which harbored six single guide RNAs (gRNAs) targeting specific sequences in the coding regions of all six genes (Supplementary Fig. 1). Using this vector, we generated ten primary T₀ lines, of which three were grown to maturity. T₁ seeds were harvested from plant 3, which showed an oval fruit phenotype, indicative of successful editing of the *ovate* locus, and determinate growth habit, indicative of loss of function of the *self-pruning* gene. Sequencing of all six targeted loci in 50 T₁ lines revealed that four of the six targeted loci were successfully edited in all 50 lines and harbored indel mutations (Supplementary Tables 2 and 3). The four edited genes were *SELF-PRUNING* (*SP*), *OVATE* (*O*), *FRUIT WEIGHT 2.2* (*FW2.2*) and *LYCOPENE BETA CYCLASE* (*CycB*). For all four edited genes, we recovered only edited alleles and did not detect any wild-type (WT) alleles in the T₁ generation (Supplementary Datasets 1 and 2). However, we did not recover any mutations in either *FASCIATED* (*FAS*) or *MULTIFLORA* (*MULT*). In the case of *FAS* we identified a G-to-A substitution in the *S. pimpinellifolium* genome at the gRNA target site (designed based on the *S. lycopersicum* genome) and the targeted *S. pimpinellifolium* sequence, which may have prevented editing (Supplementary Tables 2 and 3).

To address the specificity of our multiplex editing approach, we sequenced the two most closely related off-target loci (as determined by *in silico* analysis using Geneious R11 program) for each gRNA in two pTC321 plant 3 lines (Supplementary Fig. 2). We did not

¹Departamento de Biologia Vegetal, Universidade Federal de Viçosa, Viçosa, Brazil. ²Department of Genetics, Cell Biology and Development, Center for Genome Engineering, University of Minnesota, Minneapolis, Minnesota, USA. ³Departamento de Ciências Biológicas, Escola Superior de Agricultura “Luiz de Queiroz,” Universidade de São Paulo, Piracicaba, Brazil. ⁴Institut für Biologie und Biotechnologie der Pflanzen, Universität Münster, Münster, Germany. ⁵Instituto de Biociências, Universidade de São Paulo, São Paulo, Brazil. ⁶Present address: Inari Agriculture, Cambridge, Massachusetts, USA. ⁷These authors contributed equally to this work. Correspondence should be addressed to J.K. (jkudla@uni-muenster.de) or L.E.P.P. (lazaro.peres@usp.br).

Received 19 April; accepted 12 September; published online 1 October 2018; doi:10.1038/nbt.4272

Table 1 Known domestication genes in cereal (*maize*, *Zea mays*) and non-cereal (*soybean*, *Glycine max*) crops

Crop species	Gene target	Function	Mutation type	Genetic effect	Phenotypic outcome	Refs.
Maize	<i>Tb1</i>	TCP-family transcription factor	Retrotransposon insertion in regulatory region	Gain of function	Inhibition of side branching, altering source–sink relations and increasing yield	31,32
	<i>lg1</i>	Squamosa-promoter binding protein	Retrotransposon insertion	Loss of function	Leaf is upright due to absent ligules and auricles	28,33
	<i>tga1</i>	SBP-box transcription factor	SNP altering single amino acid	Gain of function	Changes encased to naked kernels	34
	<i>ZmCCT</i>	CCT domain-containing protein	Retrotransposon insertion in regulatory region	Loss of function	Reduction of photoperiod sensitivity	35,36
Soybean	<i>DT1</i>	CETS family of regulatory genes	SNPs altering amino acids	Loss of function	Changes growth from indeterminate to determinate, producing a shorter, more compact plant	37,38 ^a
	<i>GA2Ox</i>	Gibberellin biosynthesis enzyme	Variation in promoter region	Loss of function	Seed weight	39
	<i>SHAT1-5</i>	NAC-family transcription factor	20-bp deletion disrupting a repressive element	Gain of function	Increased secondary wall biosynthesis promoting thickening of fiber cap cells, leading to reduced shattering	40

^aActually targets the close ortholog *GmFT2*.

observe editing of either off-target locus in any of the sequenced lines (**Supplementary Dataset 1**).

Next we examined the phenotypes of two *T*₂ plant lines (designated as line 3-5 and line 3-11). The parental *T*₁ plants of both 3-5 and 3-11 contained homozygous deletions in the second exon of the gene encoding SP (**Fig. 1a**). Breeding an *sp* allele with a single nucleotide polymorphism (SNP) in the coding region into tomato cultivars was instrumental in enabling the mechanical harvest of fruits¹⁶. Similarly, loss of SP function in *S. pimpinellifolium* resulted in compact plants with reduced height, reduced number of sympodial units and determinate growth when compared with WT *S. pimpinellifolium* (**Fig. 1b–g**). In the fruit-shape-determining OVATE (*O*) locus, genome editing had induced distinct homozygous deletions in the first exon of the gene in both *T*₁ parents (**Fig. 1h**). As predicted, loss of *O* gene function in both alleles caused an oval fruit shape (**Fig. 1i–m**). The elongated form of fruits occurs through reduced internal fruit pressure and is associated with less rain-induced fruit cracking, a detrimental trait in tomato production¹⁷. In the FRUIT WEIGHT 2.2 (*FW2.2*) locus, we identified two independent homozygous deletions that disrupted the coding frame of exon 2 (**Supplementary Fig. 3**). Surprisingly, despite these mutations, we did not detect any discernible change in fruit sizes in these *T*₂ mutant lines compared with WT *S. pimpinellifolium* (**Supplementary Table 4**).

During the course of our experimental program, we learned that the gene locus responsible for the multilocular fruit phenotype of *FAS* is not encoded by a YABBY transcription factor, as was previously proposed¹⁸, but instead results from a mutation in *CLAVATA3* (*CLV3*)¹². Therefore, we carried out a second round of genome engineering to generate multiplex-edited plants in which the selection of target genes focused on modulating fruit size (*FW2.2*, *FAS*) and number (*MULT*), as well as nutritional value (*LYCOPENE BETA CYCLASE*, *CycB*). We designed a CRISPR–Cas9 plant transformation vector named pTC603 (**Supplementary Note 2**), which harbored eight gRNAs targeting two sites in the coding region of each of these four genes (**Supplementary Fig. 1**). Three successfully transformed *T*₀ lines were identified (**Supplementary Fig. 4**). Sequencing of *T*₀ plants 5 and 8 identified loss-of-function mutations in all four targeted loci in both lines (**Supplementary Fig. 5** and **Supplementary Dataset 2**). Target locus analysis in 28 individual *T*₁ representatives derived from both *T*₀ plants 5 and 8 revealed that in every *T*₁ plant all four target loci were successfully edited (**Supplementary Dataset 1**). In *CycB* and *FW2.2* we identified two different mutation events and in *CLV3* three different mutation events homozygous mutations or heterozygous (biallelic) combinations of mutant alleles. Either type of mutation resulted in a loss of function of the edited gene. For *MULT*, we recovered 5 *T*₁ plants possessing two

WT alleles and 23 heterozygous *T*₁ plants (**Supplementary Table 5**). We examined the two most closely related genomic sequences for each gRNA (as determined by *in silico* analysis using the Geneious R11 program) and did not observe off-target editing in ten analyzed *T*₁ plants (**Supplementary Fig. 2**). To summarize, in two separate experiments we engineered two sets of four target domestication genes simultaneously and generated a diverse range of combinations of 15 independent loss-of-function alleles (**Supplementary Tables 3** and **4**).

We phenotyped the second set of edited plant lines. Introduction of a loss-of-function *MULT* allele into cultivated tomato resulted in a higher number of fruits per truss, conferring enhanced yield¹⁴. In our edited plant lines, we identified a single heterozygous mutation (2-bp deletion) in exon 2 (**Fig. 2a** and **Supplementary Fig. 5**) of *MULT*. Edited plants had the predicted branched inflorescence phenotype (*T*₁, **Fig. 2b–d**; *T*₀, **Supplementary Fig. 6**). Both *T*₁ lines also harbored homozygous indel mutations in both the first and the second exon of the *FW2.2* gene (**Supplementary Fig. 5**). Moreover, *T*₁ lines 5 and 8 also carried biallelic deletions in exon 1 and a heterozygous deletion in exon 2 of the *CLV3* gene (**Fig. 2e**), which corresponded with phenotypes that have been attributed to the *FAS* locus (**Fig. 2f,g**). Characterization of fruit morphology revealed a fourfold increase in fruit locule number and a fruit weight increased up to 200% compared with *S. pimpinellifolium* (**Fig. 2h,i**). Considering the absence of a discernible fruit phenotype in the lines in which *FW2.2* but not *FAS* was mutated (**Supplementary Fig. 3** and **Supplementary Table 4**), we conclude that increased fruit size (**Fig. 2j,k**) is due to the loss of function of *CLV3*. Since the classical *fw2.2* mutation, which affects fruit size, causes a heterochronic alteration in the *FW2.2* expression pattern, we suggest that changes in *FW2.2* expression, but not loss of function, affect tomato fruit size¹³.

Nutritional value and taste have largely been neglected in conventional breeding¹⁹. The content of lycopene and β-carotene largely determines the nutritional value of tomato²⁰. Anti-inflammatory properties and the reduction of cardiovascular and cancer risks have also been correlated with dietary intake of lycopene²¹. In addition, while β-carotene occurs in sufficient amounts in many vegetables, lycopene is generally not present in sufficient concentration²². In cultivated tomato, the activity of lycopene β-cyclase converts a substantial fraction of lycopene into β-carotene, thereby reducing the content of beneficial lycopene¹⁵. While cultivated cherry tomato fruits accumulate around 60–120 mg kg⁻¹ lycopene^{23,24}, this antioxidant accumulates to levels of up to 270 mg kg⁻¹ in *S. pimpinellifolium*^{25,26}. The genetic bases determining lycopene accumulation in tomato are only poorly understood and most likely polygenic²⁷. Accordingly, previous attempts to enhance lycopene

content of commercial tomato yielded only moderate success or resulted in enhanced lycopene accumulation at the cost of reduced β -carotene abundance^{15,28}.

We targeted the *CycB* gene in both experiments to evaluate whether we could exploit the lycopene accumulation phenotype of *S. pimpinellifolium*. In all four edited *S. pimpinellifolium* lines, we detected biallelic

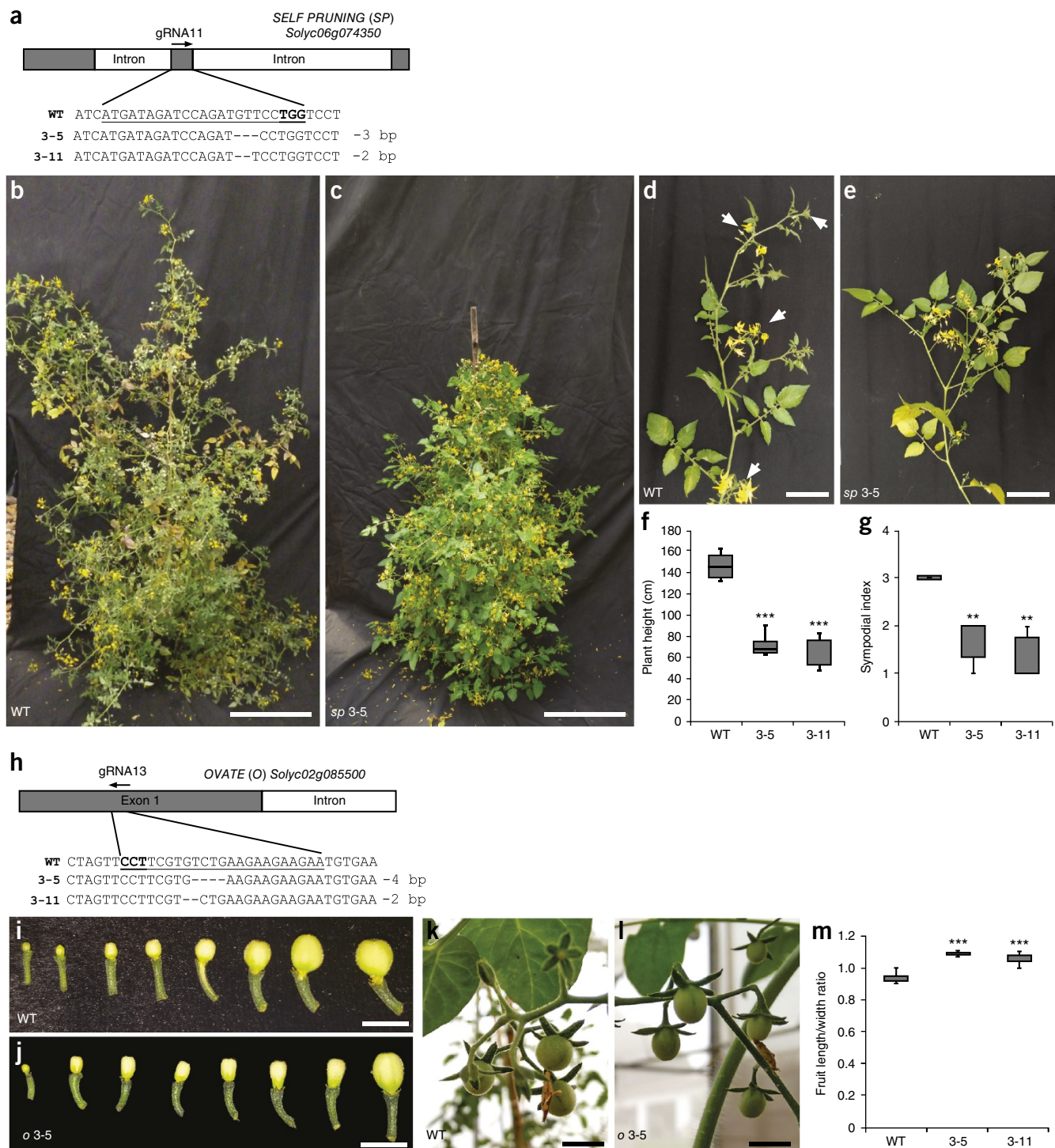


Figure 1 Plant morphology and fruit shape in *de novo* domesticated *S. pimpinellifolium* plants. (a) Genomic sequence showing the gRNA target site (underlined) and the resulting missense mutation in the *SP* gene. The PAM sequence is depicted in bold. (b,c) Representative WT (b) and T₂ *sp* mutant (c) plants with determinate growth habit; bars, 30 cm. (d,e) Detailed view of the vegetative branch with successive sympodial units (inflorescence plus three leaves; white arrows) in WT (d) and T₂ *sp* mutant (e); bars, 5 cm. (f,g) Height (f) and sympodial index (g) alterations in WT and *sp* mutant plants. (h) Genomic sequence showing the site of gRNA targeting and the resulting missense mutation in the *O* gene. (i-l) Developmental series of early fruits of WT (i) and T₂ *ovate* (j) plants (bars, 1 cm) and their respective unripe fruits in the plant (k,l); bars, 5 cm. (m) Fruit length/width ratio in WT and line 3-5 and 3-11 mutant plants. Two-tailed *t*-test (WT vs. lines): ***P* < 0.01 and ****P* < 0.001; *n* = 6 plants for height and sympodial index and *n* = 90 fruits for fruit length/width ratio. Data are depicted in box plots: box, interquartile range (IQR); whiskers, 1.5 × IQR; center line, mean.

or homozygous loss-of-function mutations in the first exon of *CycB* (Fig. 3a and Supplementary Figs. 5 and 7). These genetic alterations resulted in flowers with orange antheridial cones (due to lycopene

accumulation) rather than the yellow anthers of *S. pimpinellifolium* lines 5 and 8 (Fig. 3b-d) and resulted in deep red fruits (Fig. 3e,f). Quantitative determination of the carotenoid content in fruits of cherry

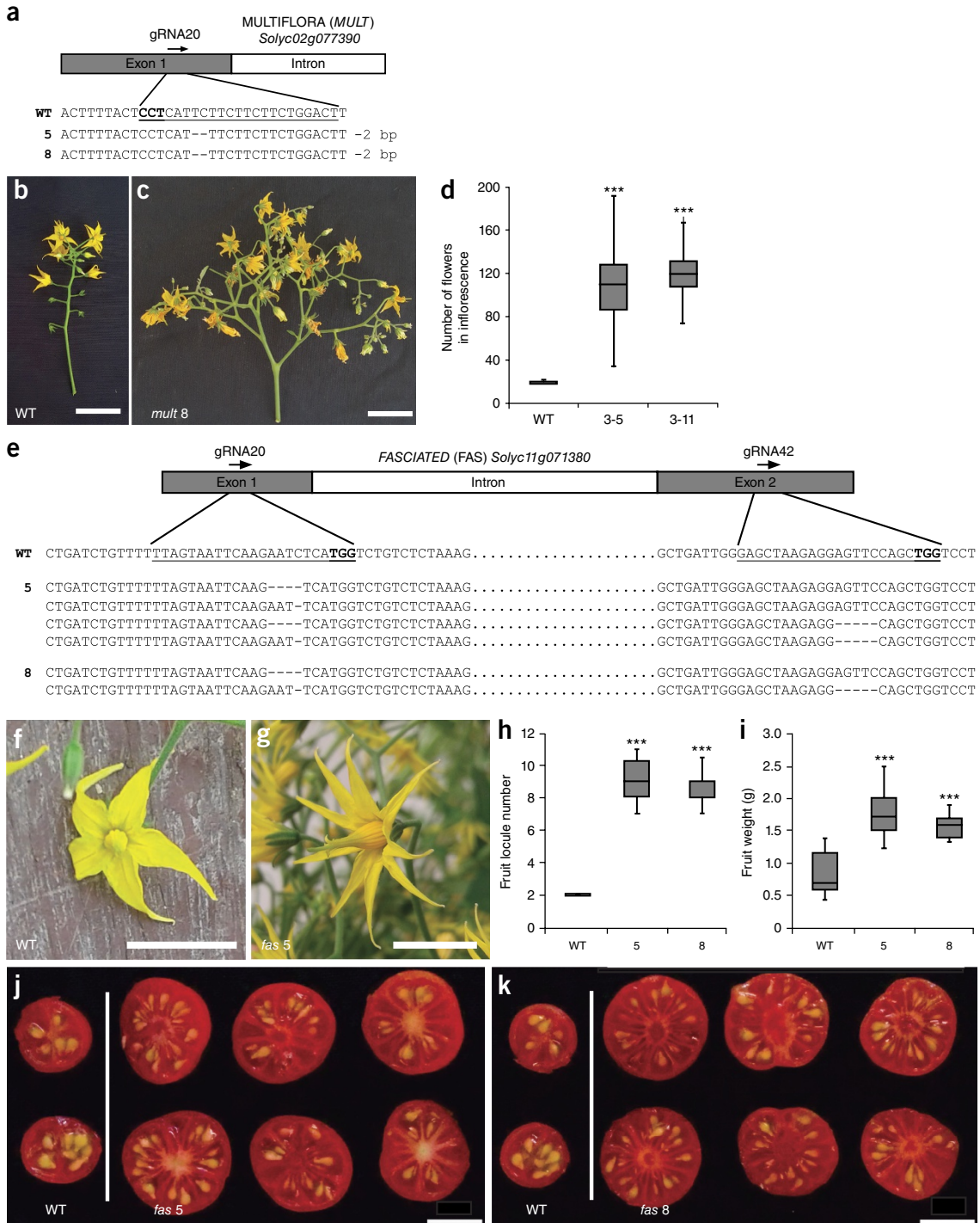


Figure 2 Flower number and fruit size in *de novo* domesticated *S. pimpinellifolium* plants. (a) *MULT* genomic sequence showing the site of gRNA targeting and the resulting missense mutations. (b,c) Representative WT (b) and T_1 *multiflora* (*mult*) (c) mutant inflorescences. Note the increased number of petals and their intense yellow color due to the mutated *fas* and *cycB* alleles targeted in the same vector. Bars, 2 cm. (d) Number of flowers per inflorescence in WT and two different T_1 mutants. (e) *clv3* genomic sequence (of the *fas* allele) showing the site of gRNA targeting and the resulting missense mutations. (f,g) Macroscopic flower morphology in WT (f) and T_1 multi-petal *fas* (g) mutant plants; bars, 2 cm. (h,i) Fruit locules (h) and weight (i) in WT and two different mutant plant lines (derived from events 5 and 8). Increased locule number led to increased fruit size in both *fas* line 5 T_1 (j) and *fas* line 8 T_1 (k) mutant plant lines. Scale bars, 1 cm. Two-tailed *t*-test (WT vs. lines): ****P* < 0.001; *n* = 60 inflorescences for flower number per inflorescence and *n* = 90 fruits for fruit locule number and weight. Data are depicted in box plots: box, IQR; whiskers, 1.5 × IQR; center line, mean.

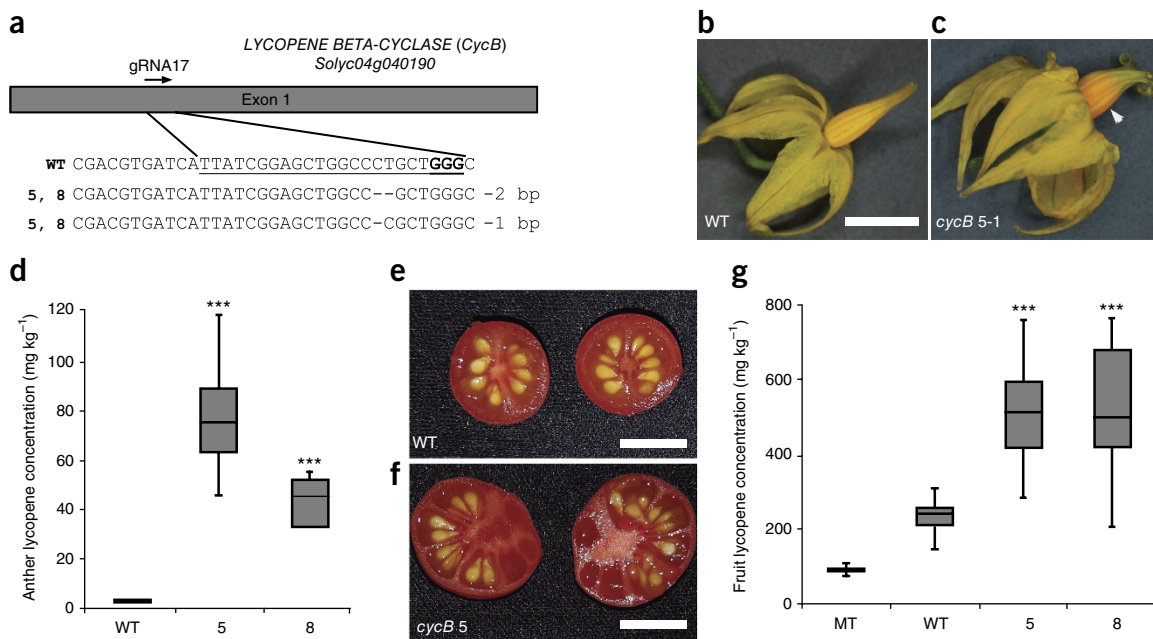


Figure 3 Nutritional content of fruits from engineered *S. pimpinellifolium* plants. (a) *CycB* genomic sequence showing the site of gRNA targeting and the resulting missense mutations in plants 5 and 8 created using vector pTC603. (b,c) Close-up of (b) WT and (c) *cycB* T₁ mutant flowers; arrowhead shows anther color alteration due to lycopene accumulation; bar, 2 cm in b,c. (d) Lycopene concentration in the antheridial cones of WT and two different T₁ mutant plant lines (derived from events 5 and 8). (e,f) Cross-sections of representative T₁ fruits showing intensification of the red color in *cycB* mutant plants; bar, 1 cm. (g) Lycopene concentration in mature fruits of cherry tomato cultivar Micro-Tom (MT), *S. pimpinellifolium* (WT) and two different *S. pimpinellifolium* mutant lines (derived from events 5 and 8). One-way ANOVA followed by Tukey's HSD test (mutants vs. WT): ***P < 0.001. n = 6 plants (pooled flowers or fruits) for lycopene content in flowers or fruits. Data are depicted in box plots: box, IQR; whiskers, 1.5 × IQR; center line, mean.

tomatoes cv. Micro-Tom (MT) and those of wild and edited *S. pimpinellifolium* lines revealed values of 92, 234, and 510 mg kg⁻¹ of lycopene, respectively (Fig. 3g and Supplementary Tables 6 and 7). This represents more than 100% higher accumulation of lycopene in the edited lines when compared with the parent species. Further, this value is more than 500% higher than concentrations commonly found in commercial cherry tomatoes^{23,24}. Importantly, this improvement in lycopene content did not negatively affect the accumulation of β-carotene or lutein (Supplementary Fig. 8).

Finally, we monitored the stability of the observed phenotypes in the T₂ (pTC603) and T₃ (pTC321) generations and verified their occurrence independent of the Cas9 transgene. Diagnostic PCR analyses identified transgene-free plants that had all of the domestication phenotypes (Supplementary Fig. 9). Important traits such as Brix value, fruit shape and locule number were uniformly inherited in the T₂ (pTC603) and T₃ (pTC321) generations (Supplementary Figs. 10 and 11 and Supplementary Tables 8 and 9).

In this report we provide evidence that targeted reverse genetic engineering of wild plants could rapidly create new crops. We demonstrate that simultaneous CRISPR–Cas9 editing of six genes resulted in modification of fruit number, size, shape, nutrient content and plant architecture in a single generation and within a single transformation experiment. Recently, a complementary promoter editing approach has been applied to create genetic variability and reverse the negative effects of domestication history in order to aid breeding of beneficial traits in tomato²⁹. Combining this synthetic genetic variability method with *de novo* domestication could boost efforts to rapidly engineer better crops. Importantly, domestication traits have also been characterized in many crops, including maize, wheat and sorghum^{6,30}, meaning that our approach could be broadly applied⁹.

METHODS

Methods, including statements of data availability and any associated accession codes and references, are available in the online version of the paper.

Note: Any Supplementary Information and Source Data files are available in the online version of the paper.

ACKNOWLEDGMENTS

We are grateful to S. Schültke for technical assistance. This work was supported by funding from the Agency for the Support and Evaluation of Graduate Education (CAPES, Brazil), the National Council for Scientific and Technological Development (CNPq, Brazil) and Foundation for Research Assistance of the São Paulo State (FAPESP, Brazil), and the German Federal Ministry of Education and Research (BMBF, Germany). We thank CAPES for scholarships granted to E.R.N. and FAPESP for the scholarship granted to M.M.N. (2013/12209-1). L.E.P.P. was supported by FAPESP grant 2013/18056-2. FAPESP and BMBF provided a grant for L.E.P.P. (2015/50220-2) and J.K. (031B0334). L.E.P.P. acknowledges a grant from CNPq (grant 307040/2014-3).

AUTHOR CONTRIBUTIONS

A.Z., T.C., D.F.V., J.K. and L.E.P.P. designed the study. A.Z., T.C., M.M.N., E.R.N., K.H.E., S.W. and L.E.P.P. performed experiments. A.Z., T.C. and K.H.E. analyzed data. A.Z., K.H.E., J.K. and L.E.P.P. prepared the manuscript. All authors have revised and approved the final version of the manuscript.

COMPETING INTERESTS

After completion of this work in the laboratory of D.F.V., T.C. became an employee of Inari Agriculture, a company that uses novel technologies for crop breeding. D.F.V. is a founder and Chief Science Officer of Calyxt, a company applying genome editing to plants.

Reprints and permissions information is available online at <http://www.nature.com/reprints/index.html>. Publisher's note: Springer Nature remains neutral with regard to jurisdictional claims in published maps and institutional affiliations.

- Evans, L.T. *Crop Evolution, Adaptation and Yield* (Cambridge Univ. Press, 1996).

2. van de Wouw, M., Kik, C., van Hintum, T., van Treuren, R. & Visser, B. Genetic erosion in crops: concept, research results and challenges. *Plant Genet. Resour.* **8**, 1–15 (2010).
3. Food and Agriculture Organization of the United Nations. *FAO Statistical Yearbook 2015: World Food and Agriculture* (United Nations, 2015).
4. Lippman, Z. & Tanksley, S.D. Dissecting the genetic pathway to extreme fruit size in tomato using a cross between the small-fruited wild species *Lycopersicon pimpinellifolium* and *L. esculentum* var. Giant Heirloom. *Genetics* **158**, 413–422 (2001).
5. Gruber, K. Agrobiodiversity: the living library. *Nature* **544**, S8–S10 (2017).
6. Meyer, R.S. & Purugganan, M.D. Evolution of crop species: genetics of domestication and diversification. *Nat. Rev. Genet.* **14**, 840–852 (2013).
7. Čermák, T. *et al.* A multipurpose toolkit to enable advanced genome engineering in plants. *Plant Cell* **29**, 1196–1217 (2017).
8. Falke, K.C. *et al.* The spectrum of mutations controlling complex traits and the genetics of fitness in plants. *Curr. Opin. Genet. Dev.* **23**, 665–671 (2013).
9. Zsögön, A., Čermák, T., Voytas, D. & Peres, L.E.P. Genome editing as a tool to achieve the crop ideotype and *de novo* domestication of wild relatives: case study in tomato. *Plant Sci.* **256**, 120–130 (2017).
10. Pnueli, L. *et al.* The SELF-PRUNING gene of tomato regulates vegetative to reproductive switching of sympodial meristems and is the ortholog of *CEN* and *TFL1*. *Development* **125**, 1979–1989 (1998).
11. Liu, J., Van Eck, J., Cong, B. & Tanksley, S.D. A new class of regulatory genes underlying the cause of pear-shaped tomato fruit. *Proc. Natl. Acad. Sci. USA* **99**, 13302–13306 (2002).
12. Xu, C. *et al.* A cascade of arabinosyltransferases controls shoot meristem size in tomato. *Nat. Genet.* **47**, 784–792 (2015).
13. Frary, A. *et al.* Fw2.2: a quantitative trait locus key to the evolution of tomato fruit size. *Science* **289**, 85–88 (2000).
14. Lippman, Z.B. *et al.* The making of a compound inflorescence in tomato and related nightshades. *PLoS Biol.* **6**, e288 (2008).
15. Ronen, G., Carmel-Goren, L., Zamir, D. & Hirschberg, J. An alternative pathway to β-carotene formation in plant chloroplasts discovered by map-based cloning of *beta* and *old-gold* color mutations in tomato. *Proc. Natl. Acad. Sci. USA* **97**, 11102–11107 (2000).
16. Rick, C.M. The tomato. *Sci. Am.* **239**, 76–87 (1978).
17. Peet, M.M. Fruit cracking in tomato. *HortTechnology* **2**, 216–223 (1991).
18. Cong, B., Barrero, L.S. & Tanksley, S.D. Regulatory change in YABBY-like transcription factor led to evolution of extreme fruit size during tomato domestication. *Nat. Genet.* **40**, 800–804 (2008).
19. Tieman, D. *et al.* A chemical genetic roadmap to improved tomato flavor. *Science* **355**, 391–394 (2017).
20. Römer, S. *et al.* Elevation of the provitamin A content of transgenic tomato plants. *Nat. Biotechnol.* **18**, 666–669 (2000).
21. Clinton, S.K. Lycopene: chemistry, biology, and implications for human health and disease. *Nutr. Rev.* **56**, 35–51 (2009).
22. Bramley, P.M. Is lycopene beneficial to human health? *Phytochemistry* **54**, 233–236 (2000).
23. Lenucci, M.S., Cadini, D., Taurino, M., Piro, G. & Dalessandro, G. Antioxidant composition in cherry and high-pigment tomato cultivars. *J. Agric. Food Chem.* **54**, 2606–2613 (2006).
24. Kuti, J.O. & Konuru, H.B. Effects of genotype and cultivation environment on lycopene content in red-ripe tomatoes. *J. Sci. Food Agric.* **85**, 2021–2026 (2005).
25. Adalid, A.M., Roselló, S. & Nuez, F. Evaluation and selection of tomato accessions (*Solanum* section *Lycopersicon*) for content of lycopene, β-carotene and ascorbic acid. *J. Food Compos. Anal.* **23**, 613–618 (2010).
26. Ashrafi, H., Kinkade, M.P., Merk, H.L. & Foolad, M.R. Identification of novel quantitative trait loci for increased lycopene content and other fruit quality traits in a tomato recombinant inbred line population. *Mol. Breed.* **30**, 549–567 (2012).
27. Liu, Y.-S. There is more to tomato fruit colour than candidate carotenoid genes. *Plant Biotechnol. J.* **1**, 195–207 (2003).
28. Li, C. *et al.* RNA-guided Cas9 as an in vivo desired-target mutator in maize. *Plant Biotechnol. J.* **15**, 1566–1576 (2017).
29. Soyk, S. *et al.* Bypassing negative epistasis on yield in tomato imposed by a domestication gene. *Cell* **169**, 1142–1155.e12 (2017).
30. Doebley, J.F., Gaut, B.S. & Smith, B.D. The molecular genetics of crop domestication. *Cell* **127**, 1309–1321 (2006).
31. Doebley, J., Stec, A. & Hubbard, L. The evolution of apical dominance in maize. *Nature* **386**, 485–488 (1997).
32. Studer, A., Zhao, Q., Ross-Ibarra, J. & Doebley, J. Identification of a functional transposon insertion in the maize domestication gene *tb1*. *Nat. Genet.* **43**, 1160–1163 (2011).
33. Moreno, M.A., Harper, L.C., Krueger, R.W., Dellaporta, S.L. & Freeling, M. *liguleless1* encodes a nuclear-localized protein required for induction of ligules and auricles during maize leaf organogenesis. *Genes Dev.* **11**, 616–628 (1997).
34. Wang, H., Studer, A.J., Zhao, Q., Meeley, R. & Doebley, J.F. Evidence that the origin of naked kernels during maize domestication was caused by a single amino acid substitution in *tg1*. *Genetics* **200**, 965–974 (2015).
35. Yang, Q. *et al.* CACTA-like transposable element in ZmCCT attenuated photoperiod sensitivity and accelerated the postdomestication spread of maize. *Proc. Natl. Acad. Sci. USA* **110**, 16969–16974 (2013).
36. Huang, C. *et al.* ZmCCT9 enhances maize adaptation to higher latitudes. *Proc. Natl. Acad. Sci. USA* **115**, E334–E341 (2018).
37. Tian, Z. *et al.* Artificial selection for determinate growth habit in soybean. *Proc. Natl. Acad. Sci. USA* **107**, 8563–8568 (2010).
38. Cai, Y. *et al.* CRISPR/Cas9-mediated targeted mutagenesis of GmFT2a delays flowering time in soya bean. *Plant Biotechnol. J.* **16**, 176–185 (2018).
39. Lu, X. *et al.* The transcriptomic signature of developing soybean seeds reveals the genetic basis of seed trait adaptation during domestication. *Plant J.* **86**, 530–544 (2016).
40. Dong, Y. *et al.* Pod shattering resistance associated with domestication is mediated by a NAC gene in soybean. *Nature Commun.* **5**, 3352 (2014).

ONLINE METHODS

Molecular cloning and plant transformation. CRISPR–Cas9 plant transformation vectors were constructed using protocols 3A and 5 of Čermák *et al.*⁷. The vector pTC321 (35S::Csy4-P2A-AtCas9, 35S::gRNA-array) expressing a Csy4 array of six gRNAs targeting *SELF PRUNING* (*Soly06g074350*), *OVATE* (*Soly02g085500*), *FRUIT WEIGHT* 2.2 (*Soly02g090730*), *LYCOOPENE BETA-CYCLASE* (*Soly04g040190*), *MULTIFLORA* (*Soly02g077390*) and *FASCIATED/YABBY* (*Soly11g071810*) was constructed by direct assembly of gRNAs into the T-DNA vector pDIRECT_22C (Addgene plasmid 91135) (see **Supplementary Table 10** for gRNA sequences). Vector pTC603 (35S::Csy4-P2A-AtCas9, CmYLCV::gRNA-array) expressing a Csy4 array of eight gRNAs targeting *FASCIATED/CLAVATA3* (*Soly11g071380*), *FRUIT WEIGHT* 2.2 (*Soly02g090730*), *MULTIFLORA* (*Soly02g077390*) and *LYCOOPENE BETA-CYCLASE* (*Soly04g040190*) was constructed in two steps. The first six gRNAs were cloned into pMOD_B2103 (Addgene plasmid 91061) and the last two gRNAs into pMOD_C2200 (Addgene plasmid 91082). The gRNA arrays in the resulting plasmids were assembled along with pMOD_A0501 (35S:Csy4-P2A-AtCas9, Addgene plasmid 91011) into the T-DNA vector pTRANS_220 (Addgene plasmid 91113). The final array contains the gRNAs in the following order: gRNAs 41 and 42 targeting *FAS/CLV3*, gRNAs 15 and 16 targeting *FW2.2*, gRNAs 19 and 20 targeting *MULTIFLORA* and gRNAs 17 and 18 targeting *CycB* (**Supplementary Fig. 1** and **Supplementary Table 10**).

The pTC321 (**Supplementary Note 1**) and pTC603 (**Supplementary Note 2**) vectors were introduced into the *Agrobacterium tumefaciens* strain LBA4404 by electroporation. Agrobacteria were cultured in 3 mL of liquid LB medium supplemented with 50 mg L⁻¹ kanamycin and 50 mg L⁻¹ rifampicin and incubated at 28 °C for 24 h at 120 r.p.m. From this culture, 500 µL were added to 50 mL of fresh LB medium with the same antibiotics as above. The culture was incubated overnight under the same conditions and then centrifuged at 2,000g for 15 min at room temperature. The pellet was resuspended in liquid Murashige and Skoog (MS) medium⁴¹ to an OD₆₀₀ of 0.25–0.3; acetosyringone was added to a final concentration of 100 µM before plant inoculation.

S. pimpinellifolium (LA1589) was transformed as previously published⁴² with the following modifications: seeds were surface-sterilized by shaking in 20 mL 30% (v/v) commercial bleach (2.7% sodium hypochlorite) supplemented with two drops of commercial detergent for 15 min, followed by three rinses with sterile water. Seeds were germinated on semi-solid MS medium (supplemented with 0.6 g/L agar) and incubated at 25 ± 1 °C in the dark for 4 d. After this period, seeds were transferred and maintained at 25 ± 1 °C under long-day conditions (16 h light/ 8 h dark) with 45 µmol photons m⁻² s⁻¹ PAR irradiance.

Leaf explants (1–2 cm²) were isolated from 2-week-old *in vitro* plants and placed with the abaxial side down onto MS medium containing 1 mg L⁻¹ *trans*-zeatin, 0.1 mg L⁻¹ indole-3-acetic acid (IAA) and 100 µM acetosyringone. Two drops of *Agrobacterium* suspension were applied per explant and plates were then incubated at room temperature for 10 min. Thereafter, excess bacterial suspension was removed, and explants were blotted dry on sterile filter paper. Plates were maintained in the dark at 25 °C for 2 d for co-cultivation. Explants were transferred to plates with MS medium containing 1 mg L⁻¹ *trans*-zeatin, 0.1 mg L⁻¹ IAA, 300 mg L⁻¹ timentin, 100 mg L⁻¹ kanamycin. After 5 weeks, shoot primordia emerging from callus tissue were isolated and transferred to shoot elongation medium (MS medium supplemented with 0.5 mg L⁻¹ *trans*-zeatin, 300 mg L⁻¹ timentin, 100 mg L⁻¹ kanamycin) to recover full plants. After acclimation, these plants were grown in a greenhouse at 30 °C/26 °C day/night temperature and 60–75% ambient relative humidity, 11.5 h/13 h (winter/summer) photoperiod, sunlight 250–350 µmol photons m⁻² s⁻¹ PAR irradiance, attained by a reflecting mesh (Aluminet, Polysack Indústrias Ltda, Leme, Piracicaba, SP, Brazil), and automatic irrigation four times a day for fruit set.

Seeds from transformed plants were germinated in 350-mL pots with a 1:1 mixture of commercial potting mix Basaplant (Base Agro, Artur Nogueira, SP, Brazil) and expanded vermiculite supplemented with 1 g L⁻¹ 10:10:10 NPK and 4 g L⁻¹ dolomite limestone (MgCO₃ plus CaCO₃). Upon appearance of the first true leaf, seedlings of each genotype were transplanted to 10-L pots containing the soil mix described above, except for NPK supplementation, which was increased to 8 g L⁻¹. After transplanting, plants were sprayed twice at 14-d

intervals with 1 g L⁻¹ Peters 20-20-20 leaf fertilizer. Acclimatized plants were pollinated by hand, producing T₁ seeds and the following generations.

Seeds and vectors are available upon request from the corresponding authors see (<https://www.uni-muenster.de/Biologie.IBBP/agkudla/Plasmids.html>).

Genotyping of T₀ and T₁ plants. The gRNA target sites were amplified by PCR directly from leaf tissue with the Phire Plant Direct PCR Master Mix following the Dilution & Storage protocol (Thermo Fisher Scientific) or from extracted genomic DNA with Phusion polymerase (New England BioLabs), using primers listed in **Supplementary Table 11**. Primers and dNTPs were removed using ExoSAP (0.5 U exonuclease I + 0.25 U FastAP thermostable alkaline phosphatase in 35 µL of PCR, incubated 30 min at 37 °C and heat-inactivated for 5 min at 95 °C) and the purified PCR products were directly sequenced. Heterozygous and biallelic mutations were identified as overlapping sequence traces. These samples were cloned and several clones sequenced to determine the sequences of individual alleles.

Off-target identification and analysis. The “Find CRISPR sites” function in Geneious R11 was used to search for off-target binding sites in *S. pimpinellifolium* genome⁴³ (https://solgenomics.net/organism/Solanum_pimpinellifolium/genome). A maximum of eight mismatches and zero indels were allowed between the on- and off-target sequences. The two top scoring off-target sites were PCR amplified and sequenced. Primers can be found in **Supplementary Table 12**.

Plant material and growth conditions. Plants were cultivated in semicontrolled conditions in a greenhouse in Viçosa (642 m asl, 20° 45' S, 42° 51' W), Minas Gerais, Brazil. Wild-type *S. pimpinellifolium* plants were grown alongside T₂ of pTC321-, T₃ of pTC321- and T₁ of pTC603-transformed plants during the months of October 2016 to January 2017, August 2017 to November 2017 and August 2017 to November 2017, respectively. For plants of generations T₃ of pTC321 and T₁ of pTC603, the main stem was trained on bamboo sticks and side branches were pruned, leaving a total of three inflorescences per plant. The greenhouse temperature ranged between 24 and 20 °C, with a 13-h/11-h (day/night) photoperiod and an average irradiance of 800 µmol photons m⁻² s⁻¹. Seeds were germinated in plastic trays with commercial substrate Tropstrato and supplemented with 1 g L⁻¹ 10:10:10 NPK and 4 g L⁻¹ dolomite limestone (MgCO₃ plus CaCO₃). Weekly foliar fertilization was carried out using 2 g/L Biofert leaf fertilizer. Upon appearance of the first true leaves, seedlings of each genotype were transplanted to 5-L pots. The new pots were filled with substrate as described above, except for the NPK supplementation, which was increased to 8 g L⁻¹. Irrigation was performed twice a day in a controlled manner, so that each vessel received the same volume of water.

Carotenoid quantification and sampling. Fruits were harvested at the ‘red ripe’ stage sequentially over a period of 2 weeks. They were cut in half and the seeds were removed, after which the fruits were immediately frozen in liquid nitrogen and stored in a freezer at -80 °C until analysis. Fruit carotenoid extraction was carried out following an adaptation of a previously published protocol⁴⁴. Frozen fruits were ground in a ball mill (Retsch, model MM400) and 200-mg aliquots subsequently collected in 2-mL microtubes. During the extraction, samples were kept cooled on ice in an environment with reduced luminosity (30–50 µmol photons m⁻² s⁻¹ irradiance). 100 µL of saturated NaCl solution (370 g/L) were added to each sample and mixed by vortexing for 30 s. 200 µL of dichloromethane were added next and mixed by vortexing. Finally, 500 µL of hexane:ethyl ether (1:1) were added and the sample homogenized by vortexing. Samples were then centrifuged (Eppendorf 5415R micro-centrifuge) (4 °C, 13,000g for 5 min). The supernatant was then collected and transferred to a 2-mL amber microtube. Addition of hexane:ethyl ether (1:1), vortex agitation, centrifugation and collection of the upper organic phase (supernatant) were repeated three times, until whitening of the samples was observed in the microtube, showing the appropriate extraction of most carotenoids. Samples were completely dried in a vacuum concentrator (CentriVap, Labconco), resuspended in 300 µL of ethyl acetate and mixed for 30 s. All supernatant fractions were combined, completely dried by vacuum, filtered through a 0.45 µm membrane filter and suspended with 100 µL of ethyl acetate. Chromatography was

carried out on Agilent Technologies series 1100 HPLC system on a normal-phase Phenomenex column (Luna C18; 250 × 4.6 mm; 5 µm particle diameter) with a flow rate of 1 mL min⁻¹ and temperature 25 °C. The mobile phase was a gradient of ethyl acetate (A) and acetonitrile:water 9:1 (v/v) (B): 0–4 min: 20% A; 4–30 min: 20–65% A; 30–35 min: 65% A; 35–40 min: 65–20% A. Eluted compounds were detected between 340 and 700 nm and quantified at 450 nm. The endogenous metabolite concentration was obtained by comparing the peak areas of the chromatograms with commercial standards (Sigma-Aldrich).

The extraction of corolla and anther samples were performed in a similar way to that of fruits, but with the following modifications: after harvesting, the samples were lyophilized and stored in a refrigerator until the extraction process. The period between freeze-drying and carotenoid extraction was less than 10 d. Lyophilized samples were ground in reaction tubes with the help of a plastic pestle. Anther samples contained on average 14 mg of dry mass, corolla samples 10 mg. Samples were rehydrated in 300 µL ultrapure water and subjected to the extraction process and HPLC quantification.

Brix determination. The total content of soluble solids in fruits (measured as Brix) was determined for the ‘red ripe’ fruits stage by means of a digital bench refractometer (Instrutherm Model RTD-45). First the apparatus was calibrated with distilled water; after drying the prism, the liquid of each fruit was placed in the prism of the refractometer and thus quantified. The Brix of each replicate (each plant) was composed of analyzes of many fruits.

Phenotypic parameters of the fruits. The phenotypic parameters of the fruits (mass, length and equatorial width) were determined using precision balances (Micronal B160) and a digital caliper (MTX) using at least 10 fruits per plant.

Statistics. The quantitative parameters studied here show continuous variation and were therefore analyzed using parametric tests: Student’s *t*-test was done on GraphPad; ANOVA and Tukey HSD tests were performed using VassarStats (<http://vassarstats.net>). Percentage data were converted to the inverse function (1/X) before analysis. All information on replication, statistical test and presentation are given in the respective figure legends.

Reporting Summary. Further information on research design is available in the **Nature Research Reporting Summary** linked to this article.

Data availability. The data supporting the findings of this study are available in the paper and the accompanying Supplementary Information files. Specifically, sequences supporting on- and off-target analyses are available in **Figures 1–3**, **Supplementary Figures 2, 3, 5 and 7**, and **Supplementary Tables 3 and 4**. Raw sequences and alignments for the above mentioned figures and tables are available in **Supplementary Datasets 1** and **2**. Complete and annotated sequences of pTC321.gb and pTC603.gb are in **Supplementary Notes 1** and **2**, respectively.

41. Pino, L.E. *et al.* The Rg1 allele as a valuable tool for genetic transformation of the tomato ‘Micro-Tom’ model system. *Plant Methods* **6**, 23 (2010).
42. Murashige, T. & Skoog, F. A revised medium for rapid growth and bio assays with tobacco tissue cultures. *Physiol. Plant.* **15**, 473–497 (1962).
43. Tomato Genome Consortium. The tomato genome sequence provides insights into fleshy fruit evolution. *Nature* **485**, 635–641 (2012).
44. Sérino, S., Gomez, L., Costagliola, G. & Gautier, H. HPLC assay of tomato carotenoids: validation of a rapid microextraction technique. *J. Agric. Food Chem.* **57**, 8753–8760 (2009).

Reporting Summary

Nature Research wishes to improve the reproducibility of the work that we publish. This form provides structure for consistency and transparency in reporting. For further information on Nature Research policies, see [Authors & Referees](#) and the [Editorial Policy Checklist](#).

Statistical parameters

When statistical analyses are reported, confirm that the following items are present in the relevant location (e.g. figure legend, table legend, main text, or Methods section).

n/a Confirmed

- The exact sample size (n) for each experimental group/condition, given as a discrete number and unit of measurement
- An indication of whether measurements were taken from distinct samples or whether the same sample was measured repeatedly
- The statistical test(s) used AND whether they are one- or two-sided
Only common tests should be described solely by name; describe more complex techniques in the Methods section.
- A description of all covariates tested
- A description of any assumptions or corrections, such as tests of normality and adjustment for multiple comparisons
- A full description of the statistics including central tendency (e.g. means) or other basic estimates (e.g. regression coefficient) AND variation (e.g. standard deviation) or associated estimates of uncertainty (e.g. confidence intervals)
- For null hypothesis testing, the test statistic (e.g. F , t , r) with confidence intervals, effect sizes, degrees of freedom and P value noted
Give P values as exact values whenever suitable.
- For Bayesian analysis, information on the choice of priors and Markov chain Monte Carlo settings
- For hierarchical and complex designs, identification of the appropriate level for tests and full reporting of outcomes
- Estimates of effect sizes (e.g. Cohen's d , Pearson's r), indicating how they were calculated
- Clearly defined error bars
State explicitly what error bars represent (e.g. SD, SE, CI)

Our web collection on [statistics for biologists](#) may be useful.

Software and code

Policy information about [availability of computer code](#)

Data collection	The data collected were basically growth measurements and carotenoid determination, which did need software to be collected.
Data analysis	Statistical analyses were performed using Excel from Windows Office v. 2010 Package. DNA analyses were performed using Geneious v. 9 or DNASTar Lasergene Version 15.

For manuscripts utilizing custom algorithms or software that are central to the research but not yet described in published literature, software must be made available to editors/reviewers upon request. We strongly encourage code deposition in a community repository (e.g. GitHub). See the Nature Research [guidelines for submitting code & software](#) for further information.

Data

Policy information about [availability of data](#)

All manuscripts must include a [data availability statement](#). This statement should provide the following information, where applicable:

- Accession codes, unique identifiers, or web links for publicly available datasets
- A list of figures that have associated raw data
- A description of any restrictions on data availability

Supplementary Information files. Specifically, sequences supporting on- and off-target analyses are available in Figure 2-4, Supplementary Figure 2, 3, 5 and 7 as

well as in Supplementary Table 3 and 5. Raw sequences and alignments for the above mentioned figures and tables are available in the Supplementary Dataset 1 and 2.

Field-specific reporting

Please select the best fit for your research. If you are not sure, read the appropriate sections before making your selection.

Life sciences Behavioural & social sciences

For a reference copy of the document with all sections, see nature.com/authors/policies/ReportingSummary-flat.pdf

Life sciences

Study design

All studies must disclose on these points even when the disclosure is negative.

Sample size	Sample size was initially determined based on the number of successful plants harbouring the target mutation. From this point, growth measurements and molecules determinations were based on statistically relevant number of repetitions for ANOVA (please see materials and methods and figure legends).
Data exclusions	No data were excluded during growth analysis and analysis of carotenoid content.
Replication	As usual in growth measurements of plants, they were grown in controlled environmental conditions and experiments were performed in different and independent group of plants.
Randomization	Two sets of plants were used depending on the genes targeted in each vector. The growth parameters and carotenoid determination were performed independently in these two set of plants.
Blinding	Data were collected in randomized samples of plants size, organ length and height and tissues for carotenoid quantification

Materials & experimental systems

Policy information about [availability of materials](#)

n/a	Involved in the study
<input type="checkbox"/>	<input checked="" type="checkbox"/> Unique materials
<input checked="" type="checkbox"/>	<input type="checkbox"/> Antibodies
<input checked="" type="checkbox"/>	<input type="checkbox"/> Eukaryotic cell lines
<input checked="" type="checkbox"/>	<input type="checkbox"/> Research animals
<input checked="" type="checkbox"/>	<input type="checkbox"/> Human research participants

Unique materials

Obtaining unique materials	There are no restrictions on availability of unique materials. Both transformation vectors used and CRISPR/Cas9 plants obtained are available for research use, upon request.
----------------------------	---

Method-specific reporting

n/a	Involved in the study
<input checked="" type="checkbox"/>	<input type="checkbox"/> ChIP-seq
<input checked="" type="checkbox"/>	<input type="checkbox"/> Flow cytometry
<input checked="" type="checkbox"/>	<input type="checkbox"/> Magnetic resonance imaging